REPORT 1291

LIFT HYSTERESIS AT STALL AS AN UNSTEADY BOUNDARY-LAYER PHENOMENON [1]

By FRANKLIN K. MOORE

SUMMARY

Analysis of rotating stall of compressor blade rows requires specification of a dynamic lift curve for the airfoil section at or near stall, presumably including the effect of lift hysteresis. Consideration of the Magnus lift of a rotating cylinder suggests performing an unsteady boundary-layer calculation to find the movement of the separation points of an airfoil fixed in a stream of variable incidence. Then consideration of the shedding of vorticity into the wake should yield an estimate of lift increment proportional to time rate of change of angle of attack. This increment is the amplitude of the hysteresis loop.

An approximate analysis is carried out according to the foregoing ideas for a 6:1 elliptic airfoil at the angle of attack for maximum lift. The assumption of small perturbations from maximum lift is made, permitting neglect of distributed vorticity in the wake. The calculated hysteresis loop is counterclockwise. The computed increment of lift coefficient is quite large, indicating appreciable unsteady lift hysteresis for a very small reduced frequency of the flow oscillation. It is assumed that to the order of this analysis, the wake begins at the separation point defined by zero shear. This assumption is questionable for unsteady flow.

Finally, a discussion of the forms of hysteresis loops is presented; and, for small reduced frequency of oscillation, it is concluded that the concept of a viscous "time lag" is appropriate only for harmonic variation of angle of attack with time at mean conditions other than maximum lift.

INTRODUCTION

The phenomena of "stall flutter" and "rotating stall," which may appear in an axial-flow compressor, both involve fluctuations in flow about blades operating near their aerodynamic stall point; that is, at an average flow incidence angle near that corresponding to maximum blade lift.

The analysis of stall flutter has been held back by uncertainty as to the dependence of airfoil lift and moment on a fluctuating incidence angle near stall. In reference 1 there was proposed an assumption of the linear aerodynamic force and moment relations appropriate to steady flow at a small angle of incidence, modified by the further assumption that, as the airfoil oscillates, the forces and moments lag behind the angular displacement of the airfoil, owing to viscous effects. Such a time lag represents an unsteady hysteresis which may provide cyclic work to amplify or maintain flutter. Perhaps the first experimental study of lift hysteresis was that of Farren (ref. 2). Halfman, Johnson, and Haley (ref. 3) and Schnittger (ref. 4) have more recently studied aerodynamic hysteresis experimentally and have presented empirical analyses of their results.

An analysis of rotating stall (e. g., that of Sears, ref. 5) also requires specification of a dynamic lift-incidence relation (or the equivalent, as in the study of Emmons, Pearson, and Grant, ref. 6, and in Marble's analysis, ref. 7). Sears has adopted Mendelson's phase-lag hypothesis, and this phase angle is an undetermined parameter of his analysis.

The concept of viscous time lag is not entirely satisfactory, however, partly because the phenomenon itself is unexplained, but chiefly because the concept obviously cannot describe a lift-hysteresis loop which might occur at a nominal condition of maximum lift.

The phenomenon of aerodynamic hysteresis presumably depends, at least in part, on the airfoil boundary layer. Also, in this study, hysteresis is taken to be a fundamentally unsteady phenomenon, not explainable by consideration of the steady or quasi-steady boundary layer.[2] In the present report, consideration is given to the incompressible flow field about a single airfoil fixed in a flow of oscillating incidence, under the assumption of an unsteady but nearly quasi-steady [3] laminar boundary layer. (This sort of boundary layer is analyzed in ref. 8.) The analysis of this flow field is undertaken in order to gain an understanding of the cause of lift hysteresis and to describe its form and (crudely) its magnitude for a special airfoil at maximum lift.

The basic quasi-steady flow to be used in the present analysis is provided by Howarth's analysis (ref. 9) of the way the laminar boundary layer (and, hence, circulation) about an infinite elliptic cylinder depends on angle of attack, applied at a condition of maximum lift. In reference 9, assumptions are made under which the result becomes quantitatively inaccurate, though both the approach and the result are qualitatively instructive. The same limitations affect the present analysis.

Holding the airfoil fixed while the flow direction oscillates, simulates the accepted picture of rotating stall, in which successive blade passages stall progressively along a perfectly rigid cascade. The somewhat different case of an

[1] Supersedes NACA TN 3571, "Lift Hysteresis at Stall as an Unsteady Boundary-Layer Phenomenon," by Franklin K. Moore, 1955.

[2] Airfoils with lift curves that break sharply at stall may show lift hysteresis in steady flow, a phenomen distinct from that under study herein.

[3] In a quasi-steady flow, quantities vary slowly enough so that steady-state results apply at each instant of time although slight variations are permitted from one instant to the next.

oscillating airfoil in a uniform stream, which is appropriate to the stall flutter problem, is not analyzed in this report. However, there is an example in the "oscillating airfoil" category which illustrates the considerations underlying the present study; namely, the rotating circular cylinder in a uniform stream. If a circular cylinder is fixed in a uniform stream, it, of course, experiences no lift. Further, if it is given an angular displacement, its lift does not change, but remains zero. Thus, this degenerate "airfoil" may be said to be in a stall condition, at maximum lift, in fact. Now, if the circular cylinder is given a constant angular velocity of rotation about its axis, then a circulation develops and an aerodynamic force (Magnus force) transverse to the flow direction is exerted. If the stream velocity is from left to right and the rotation is clockwise, then the force is upward (lift). If the rotation is counterclockwise, the force is downward.

This phenomenon is explained (ref. 10, par. 27) by consideration of the boundary layer. In the case of clockwise rotation, the upper surface of the cylinder is moving with, and the bottom surface against, the flow. Consequently, if circulation remains zero, the boundary layer separates later on the top and sooner on the bottom than is the case when the cylinder is not rotating. On the top, later separation means that the velocity outside the boundary layer is lower at separation. Now, the separation point signifies the beginning of a wake. Therefore, the clockwise vorticity shed into the wake, being proportional to the local outer velocity, is less on the top, and the counterclockwise vorticity shed at the bottom separation is greater, than in the case of no rotation.

Therefore, owing to clockwise rotation, a net increase of counterclockwise vorticity is shed. By the law of conservation of circulation, the circulation therefore cannot be zero, and a clockwise circulation must develop about the airfoil to compensate for the shed vorticity. According to classical hydrodynamics, this circulation results in lift.

If, instead of rotating steadily, the cylinder undergoes a rotational oscillation, the same considerations apply, if the reduced frequency of oscillation is small. In that case, the oscillating lift is proportional to the instantaneous velocity of rotation. Thus, when the "angle of attack" of the cylinder is increasing, there is positive lift, and when the angle is decreasing, there is negative lift; over a complete cycle, the curve of lift against angle of attack would be a loop.

Therefore, the circular cylinder undergoing a rotational oscillation exhibits lift hysteresis, by reason of the response of the boundary layer to the movement of the surface. In the more complicated problem of a noncircular cylinder, or airfoil, similar considerations may be expected to apply. Of course, in the airfoil problem contemplated in the present study, the acceleration of the flow field may be expected to provide an additional component of pressure lift, derivable from consideration of Kelvin's impulse.

PRELIMINARY CONSIDERATIONS

STATEMENT OF PROBLEM

Consideration is given to the lift of an isolated airfoil in the form of an infinite elliptic cylinder with a semichord l and a thickness ratio β, at a stalling angle of attack α to a stream of velocity U (see fig. 1). A full list of notation is provided in the appendix.

While the airfoil position and the magnitude of U are held fixed, the angle of attack α is permitted to vary with time. Such a flow may be constructed by allowing a moving source Q to approach an airfoil fixed in an otherwise uniform

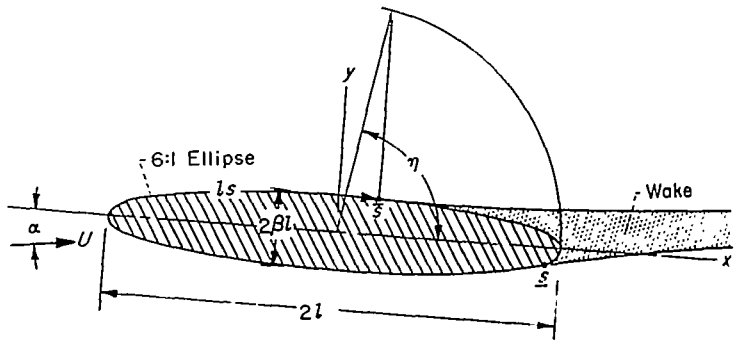

FIGURE 1.—Notation and coordinate system for elliptic airfoil at angle of attack.

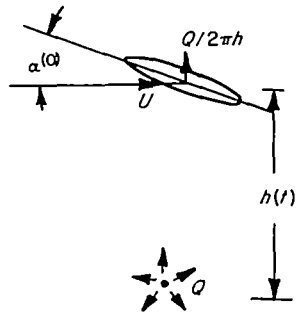

(a)

Sketch (a) Airfoil and source.

stream, the direction of approach being normal to the stream direction, as in sketch (a):

As long as h, the instantaneous distance from Q to the airfoil, is much greater than l, the airfoil finds itself effectively in a uniform stream of incidence

$$\alpha=\alpha^{(\infty)}+\frac{Q}{2\pi hU}$$

and of magnitude differing from U only to second order in $Q/2\pi hU$. The rate of change of angle of attack is

$$\dot{\alpha}=\frac{Q}{2\pi h^2U}(-\dot{h})$$

where the dot signifies differentiation with respect to time. The foregoing model applies qualitatively to the phenomenon of rotating compressor stall, if the moving source Q is taken to represent the approach of a flow blockage propagating along a cascade.

The present analysis will be carried out as though $\dot{\alpha}$ is a small constant. Actually, if $\dot{\alpha}$ is quite small, and higher derivatives such as $\ddot{\alpha}$ are negligibly small, the analysis will be correct at each instant using the appropriate instantaneous value of $\dot{\alpha}$. (This is the first refinement over the quasi-steady assumption which uses instantaneous values of α

itself; or for oscillatory α, the linear term of a Taylor series in reduced frequency.) It is clear that the solution of the problem to order $\dot{\alpha}$ provides a measure of hysteresis: Suppose an expression for lift is obtained in the form

$$C_L=C_L^{(\alpha)}+\Delta\alpha C_{L_\alpha}+\dot{\alpha}C_{L_{\dot{\alpha}}}+\ \ldots$$

The first two terms are the quasi-steady contributions. The term in $\dot{\alpha}$ provides that, if α is in the process of increasing with time, then the lift is higher (assuming $C_{L_{\dot{\alpha}}}$ positive) than the quasi-steady value. The converse is true if α is decreasing. Thus, if α performs an harmonic oscillation, the lift curve is a loop lying to either side of the quasi-steady curve of width proportional to the frequency of oscillation.

In order that the present analysis bear on the question of rotating stall, nominal angle of attack must be selected for which the airfoil is in a stalled condition. Maximum lift is the most simply described stall condition. Accordingly, the nominal angle of attack is chosen as that for which the lift is a maximum. This selection is made for two more compelling reasons:

(1) The result will tend to isolate the effect of hysteresis, inasmuch as no quasi-steady change in lift results from change in α about the maximum lift value. Of course, if lift hysteresis is found under a mean condition of maximum lift, then the idea of viscous time lag will thereby be shown to be inappropriate.

(2) Any other assumption would lead to great theoretical complication. The analysis is to be a perturbation of quasi-steady flow. If, at the nominal angle of attack, change in α resulted in a quasi-steady change in circulation, then, to the order of the present analysis, induced wake effects would require consideration.

POTENTIAL FLOW

Outside the boundary layer of the ellipse, irrotational incompressible flow is assumed. At each instant,[4] the velocity potential on the surface of the ellipse is (ref. 11, par. 71)

$$\varphi=lU(1+\beta)\cos(\eta-\alpha)-\frac{\Gamma\eta}{2\pi} \tag{1}$$

where the surface is defined by

$$x\equiv l\cos\eta;\ y\equiv\beta l\sin\eta \tag{2}$$

Along the surface, measuring s clockwise,

$$u_1=\frac{\partial\varphi}{\partial s}=\frac{\partial\varphi}{\partial\eta}\frac{\partial\eta}{\partial s}$$

$$\frac{d\eta}{ds}=-(\sin^2\eta+\beta^2\cos^2\eta)^{-1/2}\equiv-\frac{1}{R} \tag{3}$$

$$q\equiv\frac{u_1}{U}=\frac{1}{R}\left[(1+\beta)\sin(\eta-\alpha)+\frac{\Gamma}{2\pi Ul}\right] \tag{4}$$

At this juncture, the condition of maximum lift has not been imposed, and the circulation Γ is left unspecified. Of course, both α and Γ may vary with time.

The foregoing description of the potential velocity distribution is made on the assumption that the boundary layer is negligibly thin everywhere on the ellipse. This assumption is usually quite proper ahead of the separation points. The assumption that the wake aft of separation does not importantly affect the potential flow is not proper; certainly, this assumption is quantitatively poor at maximum lift, especially if the potential flow is used to compute separation point. However, the results obtained on the basis of this assumption are expected to have qualitative validity.

BOUNDARY-LAYER ANALYSIS

QUASI-STEADY BOUNDARY LAYER

As a basis for subsequent calculation of unsteady effects, the quasi-steady laminar boundary layer on the ellipse may be approximately determined by the Kármán-Pohlhausen integral method, as improved by Holstein and Bohlen (see ref. 12, ch. XII). The differential equation is

$$\frac{dZ}{ds}=\frac{F(\kappa)}{q};\quad \kappa\equiv Z\frac{dq}{ds} \tag{5a}$$

subject to the initial condition at the stagnation point ($q=0$):

$$\kappa_0=0.0770 \tag{5b}$$

where $Z=\theta^2U/\nu l$, θ being the momentum thickness. The function $F(\kappa)$ is tabulated in reference 12.

Determination of Z and Γ at maximum lift.—Given the velocity distribution q, the growth of the boundary layer may be computed from equations (5), the calculation proceeding until both the separation points ($\bar{s}$ and $\underline{s}$, fig. 1) are reached, for which $(\kappa)_{\underline{s}}=(\kappa)_{\bar{s}}=-0.1567$.

In the present problem the potential velocity distribution has not yet been fully prescribed, since Γ remains unknown. Suppose that, for a given α, a value of Γ is assumed, and the boundary-layer calculation is carried out (ref. 9). Then, at the top separation point, clockwise vorticity is shed into the wake at the rate

$$\int_0^\delta u\frac{\partial u}{\partial n}\,dn=\frac{1}{2}(u_1^2)_{\bar{s}} \tag{6}$$

while at $\bar{s}$, counterclockwise vorticity is shed at the rate $\frac{1}{2}(u_1^2)_{\underline{s}}$. Now, if $(u_1)_{\underline{s}}$ differs from $(u_1)_{\bar{s}}$, there is a net change of circulation in the wake, which is impossible in steady flow. Therefore, new trial values of Γ must be assumed until the particular value of Γ is determined for which the solution of equations (5) yields separation points for which $(u_1)_{\underline{s}}=(u_1)_{\bar{s}}$.

The foregoing procedure must be carried out for each of a number of angles of attack in order to determine the values of α and Γ at maximum lift. In reference 9, Howarth performed these calculations for $\beta=1/6$ and determined a theoretical lift curve. The maximum value of $\Gamma/2\pi Ul$ was found to be 0.0761 at an angle of attack $\alpha=7°$. His complete distribution of Z at this condition is not presented in reference 9.

[4]The quasi-steady assumption applies precisely for the calculation of the unsteady velocity potential.

Accordingly, the calculation has been repeated by integrating equation (5a) in the form

$$\frac{dZ}{d\eta}=A(\eta)F(\kappa); \quad \kappa\equiv a(\eta)Z \tag{7a}$$

where

$$A(\eta)\equiv -\frac{R}{q}; \quad a(\eta)\equiv -\frac{q_\eta}{R} \tag{7b}$$

and, from equation (4),

$$q=\frac{1}{R}\left[\frac{7}{6}\sin(\eta-7°)+0.0761\right] \tag{8}$$

At the forward stagnation point where $q=0$, $\eta_0=190.74°$, and the initial condition is, from equations (5), (6), and (7a),

$$Z_0=0.0770/a_0=0.00407 \tag{7c}$$

The solution was obtained using a step-by-step method in which a parabola is passed through two known values and the next unknown value of $dZ/d\eta$, integrating to find Z in terms of the unknown $dZ/d\eta$, then applying equation (7a) at the unknown point to solve for $dZ/d\eta$. Two starting values were found from a Taylor series about η_0. The step size in η was 10° except near the stagnation and separation point where finer spacing was used. The solution of Z is shown in figure 2 and in table I. The separation points, for which $\kappa=-0.1567$, occurred at $\eta=80.0°$ and 340.83°. Of course, q should be the same at $\bar{s}$ and $\underline{s}$. The difference cited in the table indicates the degree of error present in the calculations.

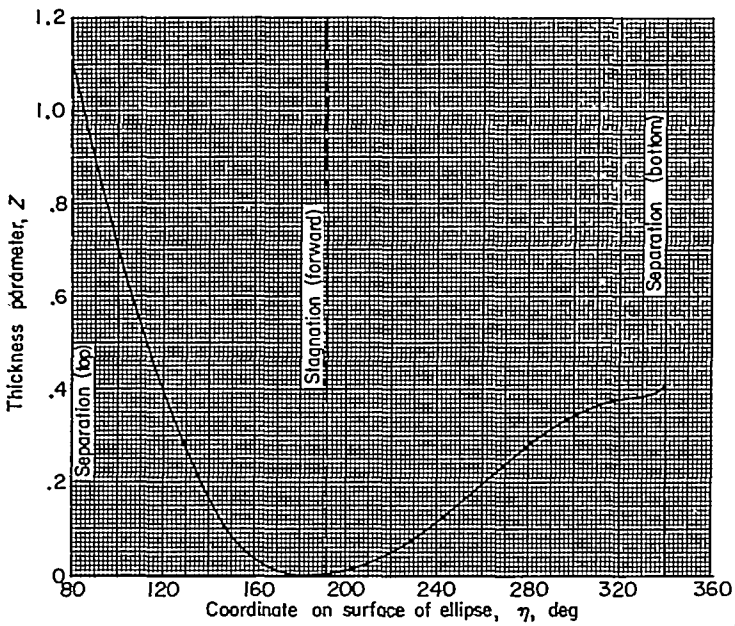

FIGURE 2.—Distribution of thickness parameter Z around ellipse.

Determination of $\partial Z/\partial\alpha$.—For subsequent use in the unsteady equations, it is necessary to know the rate of change of Z with α in quasi-steady flow. At maximum lift, when α is changed, the quasi-steady boundary layer changes, and the locations of the separation points are changed. Of course, the velocities at $\underline{s}$ and $\bar{s}$ must remain equal, because $\partial\Gamma/\partial\alpha=0$ at maximum lift, by definition.

Differentiating equation (7a) yields

$$\frac{dZ_\alpha}{d\eta}=B(\eta)Z_\alpha+b(\eta) \tag{9a}$$

where

$$\left.\begin{aligned} B&\equiv\frac{q_\eta}{q}F'(\kappa)\\ b&\equiv -A\left(\frac{q_\alpha}{q}F+\frac{Zq_{\alpha\eta}}{R}F'\right)\end{aligned}\right\} \tag{9b}$$

The initial condition for Z_α at η_0 is determined by specifying that $dZ_\alpha/d\eta$ must be finite there; from equations (9a) and (9b),

$$(Z_\alpha)_0=\left(\frac{Z_\eta q_\alpha-Zq_{\alpha\eta}F'}{q_\eta F'}\right)_0=-0.00660 \tag{9c}$$

In equations (9) all quantities are to be evaluated at the condition of maximum lift; the appropriate superscript (0) is omitted for brevity. Of course, for purposes of finding q_α and $q_{\alpha\eta}$ in equations (9), the angle of attack of 7° should be replaced by α in equation (8) and set equal to 7° again, subsequent to differentiation. Equations (9) have been integrated to yield Z_α, by the same method as described for finding Z, and the result is shown in figure 3 and in table I.

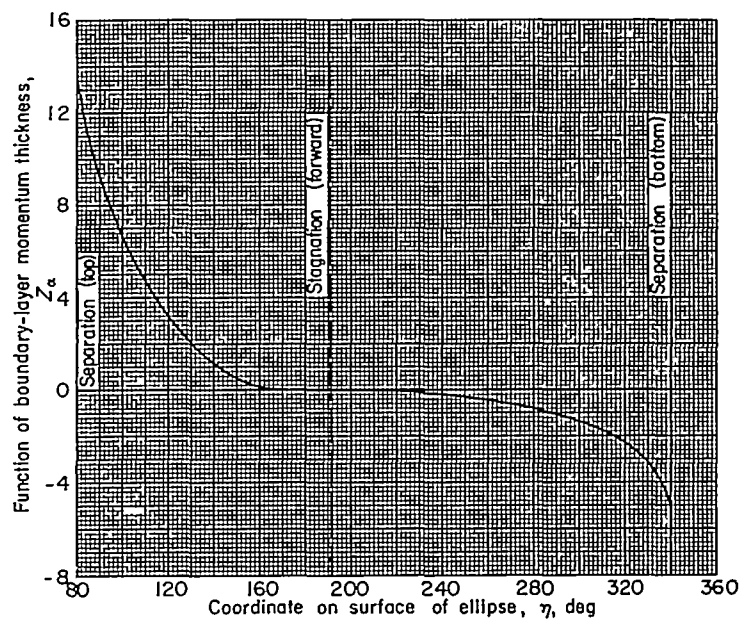

FIGURE 3.—Distribution of derivative Z_α around ellipse.

UNSTEADY BOUNDARY LAYER

The next step in the analysis is to determine the dependence of the boundary layer on the angular velocity $\dot{\alpha}$, assumed small. To this order of approximation, equation (8) describing the potential flow must be modified to include the possibility of a contribution to circulation in proportion to $\dot{\alpha}$ (or, in dimensionless form, $\epsilon\equiv\dot{\alpha}l/U$), as follows:

$$q\equiv\frac{u_1}{U}=\frac{1}{R}\left[\frac{7}{6}\sin(\eta-7°)+0.0761+\gamma\epsilon\right] \tag{10}$$

The coefficient of circulation hysteresis γ must be found from a condition of vorticity shedding at the separation points of the unsteady boundary layer. The contribution to lift proportional to $\dot{\alpha}$ then follows. Determination of the proper vorticity-shedding condition will be discussed in a subsequent section.

The unsteady form of the Kármán momentum equation (see ref. 12) is

$$\frac{\tau}{\rho}-u_1^2\frac{\partial\theta}{\partial s}-(2\theta+\delta^*)u_1\frac{\partial u_1}{\partial s}=\frac{\partial}{\partial t}(u_1\delta^*) \tag{11}$$

Steady equations (5a) and (7a) are obtained from equation (11) by omitting the term on the right side. An iteration procedure might then be adopted: The quasi-steady δ^* can be substituted into the right side of equation (11), and a new solution obtained, to include first-order unsteady effects. Using the definitions of reference 12, and writing the time derivative in equation (11) as

$$\frac{\partial}{\partial t}(u_1\delta^*)=\dot{\alpha}\frac{\partial}{\partial\alpha}(u_1\delta^*) \tag{12}$$

there is found, corresponding to equation (5a),

$$\frac{dZ}{ds}=\frac{F(\kappa)}{q}-2\frac{\epsilon}{q}f_1Z\left(\frac{q_\alpha}{q}+\frac{1}{2}\frac{Z_\alpha}{Z}+\frac{f_1'}{f_1}\kappa_\alpha\right) \tag{13}$$

The function $f_1(\kappa)$ is tabulated in reference 12, and q is given by equation (10). Again, for purposes of finding q_α and $q_{\alpha\eta}$, the angle 7° in equation (10) should temporarily be replaced by α.

Instead of the indicated iteration, in the present study the equivalent procedure is adopted of finding the coefficients of the expansion

$$Z=Z^{(0)}+\Delta\alpha Z_\alpha+\epsilon Z_\epsilon+\ \ldots$$

The coefficients $Z^{(0)}$ and Z_α have already been found (eqs. (7) and (9) and figs. 2 and 3). The derivative Z_ϵ remains to be found. Differentiating equation (13) and noting that $\kappa_\alpha=q_sZ_\alpha+q_{\alpha s}Z$,

$$\frac{dZ_\epsilon}{ds}=F'(\kappa)\frac{q_s}{q}Z_\epsilon+F'\frac{q_{\epsilon s}}{q}Z-\frac{Fq_\epsilon}{q^2}-2\frac{f_1Z}{q}\left[\frac{q_\alpha}{q}+\frac{Z_\alpha}{2Z}+\frac{f_1'}{f_1}(q_sZ_\alpha+q_{\alpha s}Z)\right] \tag{14}$$

In equation (14) and hereinafter, evaluation of quantities in the steady state at maximum lift is to be understood, and the superscript (0) is omitted for brevity.

It is impossible to ensure a finite value of dZ_ϵ/ds at the stagnation point because of the second-order pole $-2f_1Zq_\alpha/q^2$. The physical reason for this result is the fact that, at the stagnation point of a certain instant, the boundary-layer velocity profile will not vanish, as in steady flow, but rather will respond to the instantaneous acceleration ϵ more promptly than the outer potential flow. A profile of magnitude ϵ may thus be expected, vanishing in the outer stream as well as the wall as shown in sketch (b):

Therefore, the definition of momentum thickness

$$\theta\equiv\int_0^\infty\frac{u}{u_1}\left(1-\frac{u}{u_1}\right)dy$$

shows that, if the velocity u in the boundary layer has a part proportional to u_1 and a part proportional to ϵ, then the part of θ (and hence of $Z=\theta^2U/\nu l$) which is proportional to ϵ must have a simple pole in u_1. Actually, of course, the quantity θ is inappropriate for defining a thickness of a profile of the type shown in sketch (b), and the appearance of a pole in θ simply indicates this lack of physical significance.

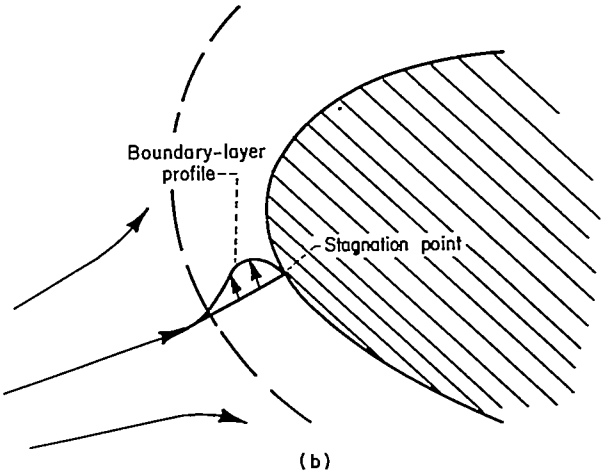

(b)

Sketch (b) Nose of airfoil.

The foregoing considerations suggest that a new variable W be defined to replace Z_ϵ:

$$W=qZ_\epsilon \tag{15}$$

Substituting equation (15) into equation (14) yields

$$\frac{dW}{ds}=\frac{q_s}{q}(1+F')W+ZF'q_{\epsilon s}-F\frac{q_\epsilon}{q}-2f_1Z\left[\frac{q_\alpha}{q}+\frac{Z_\alpha}{2Z}+\frac{f_1'}{f_1}(q_sZ_\alpha+q_{\alpha s}Z)\right] \tag{16}$$

In order that dW/ds be finite at the stagnation point, the two poles on the right side of equation (16) must cancel, yielding the initial condition

$$W_0=\left[\frac{2f_1Zq_\alpha}{(1+F')q_s}\right]_0=-0.001015 \tag{17}$$

where the numerical value is obtained using equations (3), (7c), and (10), and the tables of reference 2. Inasmuch as $q_\epsilon=\gamma/R$ (eq. (10)), the function W may be split into two parts, as follows:

$$W\equiv X+\gamma Y \tag{18}$$

so that (changing to η as independent variable) equations (16) and (17) provide

$$\frac{dX}{d\eta}=C(\eta)X+c(\eta) \tag{19a}$$

where

$$\left.\begin{aligned} C(\eta)&\equiv(1+F')\frac{q_\eta}{q} \\ c(\eta)&\equiv 2f_1RZ\left[\frac{q_\alpha}{q}+\frac{Z_\alpha}{2Z}-\frac{f_1'}{Rf_1}(q_\eta Z_\alpha+q_{\alpha\eta}Z)\right]\end{aligned}\right\} \tag{19b}$$

and

$$X_0=-0.001015 \tag{19c}$$

$$\frac{dY}{d\eta}=C(\eta)Y+d(\eta) \tag{20a}$$

where

$$d(\eta)\equiv\frac{F}{q}-ZF'\frac{R_\eta}{R^2} \tag{20b}$$

and

$$Y_0=0 \tag{20c}$$

Equations (19b) and (20b) are evaluated using the solutions for Z and Z_α, the tables of reference 12, and equations (3) and (10).

Solutions of equations (19) and (20), obtained by the method used to find Z, are presented in figures 4 and 5 and table I.

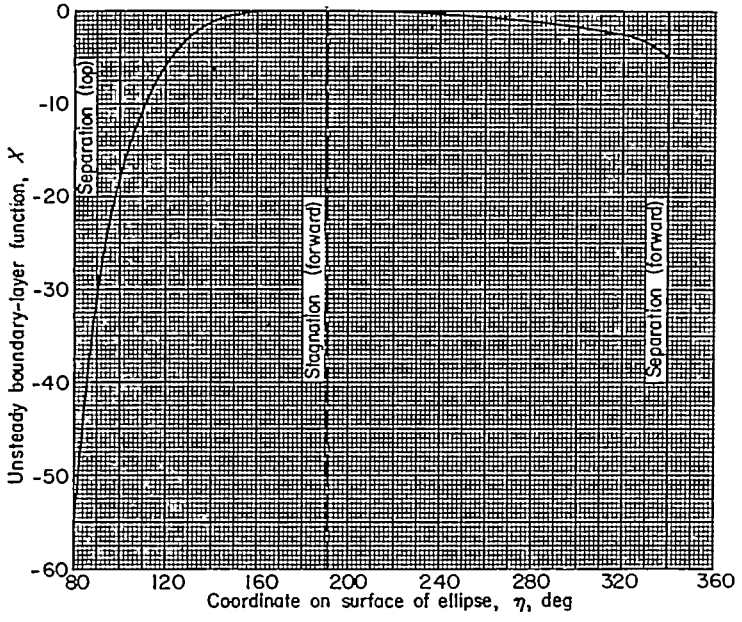

FIGURE 4.—Distribution of parameter X of unsteady boundary layer.

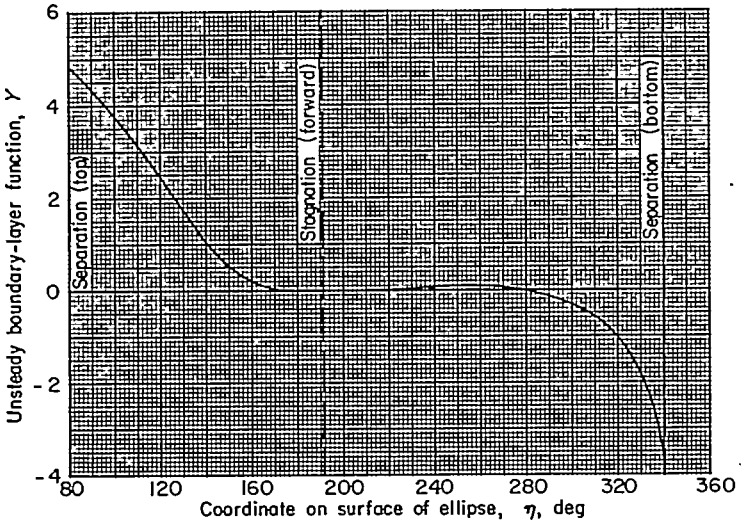

FIGURE 5.—Distribution of parameter Y of unsteady boundary layer.

DETERMINATION OF LIFT

UNSTEADY BALANCE OF SHED VORTICITY

In order to determine the unsteady pressure lift, the coefficient γ (eq. (10)) must be determined. In steady flow (see the discussion accompanying eq. (6)), the circulation Γ was obtained by requiring that vorticity be shed in equal and opposite amounts at the two separation points.

In the present unsteady problem, the net rate of vorticity appearance in the wake must vanish, not only in the quasi-steady approximation, but to order $\dot{\alpha}$ as well, in view of the assumption that the quasi-steady circulation is maximum. By the classical theorem concerning constancy of circulation, any net rate of discharge of vorticity into the wake must be balanced by a rate of increase of circulation about the body. If the airfoil is nominally at maximum lift, then the circulation terms (eq. (10)), to order $\epsilon\equiv\dot{\alpha}l/U$, are

$$0.0761+\gamma\epsilon$$

The rate of increase of this expression is at most of order $\ddot{\alpha}$, and therefore there cannot be any net discharge of vorticity to order $\dot{\alpha}$.

If the airfoil were not at maximum lift, then the expression for circulation would contain a term proportional to $\Delta\alpha$, which would change at the rate $\dot{\alpha}$, and would have to be balanced by a net rate of vorticity discharge of order $\dot{\alpha}$. In turn, this distribution of circulation in the wake would induce further modifications of the potential flow. Therefore, the assumption of maximum lift permits the neglect of the induced effects of distributed circulation in the wake.

Movement of separation points.—In order to effect a balance (to order $\dot{\alpha}$) of vorticity shed at the separation points, the movements of the separation points must be taken into account. The position of the top separation point $\bar{s}$ may be written

$$\bar{\eta}=(\bar{\eta})_{\bar{s}}+\Delta\alpha\left(\frac{\partial\bar{\eta}}{\partial\alpha}\right)_{\bar{s}}+\epsilon\left(\frac{\partial\bar{\eta}}{\partial\epsilon}\right)_{\bar{s}}+\cdots \tag{21}$$

The coefficient $\left(\frac{\partial\bar{\eta}}{\partial\alpha}\right)_{\bar{s}}$ is obtained from the quasi-steady solution:

At separation ($\kappa=-0.1567$),

$$\left(\frac{\partial\bar{\eta}}{\partial\alpha}\right)_{\bar{s}}=-\left(\frac{\partial\kappa/\partial\alpha}{\partial\kappa/\partial\eta}\right)_{\bar{s}}$$

From equations (7),

$$\frac{\partial\kappa}{\partial\eta}=-\frac{1}{R}\left(Zq_{\eta\eta}+Z_\eta q_\eta+\frac{35\kappa}{72R}\sin 2\eta\right) \tag{22a}$$

$$\frac{\partial\kappa}{\partial\alpha}=-\frac{1}{R}(Zq_{\eta\alpha}+Z_\alpha q_\eta) \tag{22b}$$

whence, holding κ fixed at -0.1567,

$$\left(\frac{\partial\bar{\eta}}{\partial\alpha}\right)_{\bar{s}}=-\left(\frac{Zq_{\eta\alpha}+Z_\alpha q_\eta}{Zq_{\eta\eta}+Z_\eta q_\eta+\frac{35\kappa}{72R}\sin 2\eta}\right)_{\bar{s}} \tag{23}$$

where Z and Z_α may be obtained from table I.

The coefficient $(\partial\bar{\eta}/\partial\epsilon)_{\bar{s}}$ comes from the unsteady solution:

$$\left(\frac{\partial\bar{\eta}}{\partial\epsilon}\right)_{\bar{s}}=-\left(\frac{\partial\kappa/\partial\epsilon}{\partial\kappa/\partial\eta}\right)_{\bar{s}}$$

From equations (7),

$$\kappa_\epsilon=-\frac{1}{R}\left(Z_\epsilon q_\eta+Z q_{\eta\epsilon}\right)$$

which, upon substitution of equations (10), (15), and (18), becomes

$$\kappa_\epsilon=-\frac{1}{R}\left(X+\gamma Y\right)\frac{q_\eta}{q}+\frac{35Z\gamma}{72R^4}\sin 2\eta \tag{24}$$

Equations (22a) and (24) thus provide that

$$\left(\frac{\partial\bar{\eta}}{\partial\epsilon}\right)_{\bar{s}}=-\left[\frac{X\frac{q_\eta}{q}+\gamma\left(Y\frac{q_\eta}{q}-\frac{35Z}{72R^3}\sin 2\eta\right)}{Zq_{\eta\eta}+Z_\eta q_\eta+\frac{35\kappa}{72R}\sin 2\eta}\right]_{\bar{s}} \tag{25}$$

At the bottom stagnation point, equations (21), (23), and (25) apply, with subscript $\underline{s}$ replacing subscript $\bar{s}$.

Equation of vorticity shed at separation points.—Taking into account the motion of the separation point, the rate of vorticity shedding at the top is given by the following equation, which replaces equation (6):

$$\int_0^\delta\left(\bar{u}-l\frac{d\bar{s}}{dt}\right)\frac{\partial\bar{u}}{\partial n}\,dn=\frac{1}{2}\bar{u}_1^2-l\frac{d\bar{s}}{dt}\bar{u}_1 \tag{26}$$

From equations (3) and (21),

$$\left.\begin{aligned}&\frac{d\bar{s}}{dt}=-R\frac{\partial\bar{\eta}}{\partial t}=-\dot{\alpha}\left(R\frac{\partial\bar{\eta}}{\partial\alpha}\right)_{\bar{s}}+\ldots=-\frac{U}{l}\epsilon\left(R\frac{\partial\bar{\eta}}{\partial\alpha}\right)_{\bar{s}}+\ldots\\&\bar{u}_1=(u_1)_{\bar{s}}+\left(\frac{\partial u_1}{\partial n}\right)_{\bar{s}}\left[\Delta\alpha\left(\frac{\partial\bar{\eta}}{\partial\alpha}\right)_{\bar{s}}+\epsilon\left(\frac{\partial\bar{\eta}}{\partial\epsilon}\right)_{\bar{s}}\right]+\ldots\end{aligned}\right\} \tag{27}$$

Equations (27) yield the following expression for the right side of equation (26):

$$\frac{1}{2}(u_1^2)_{\bar{s}}+(u_1)_{\bar{s}}\left[\Delta\alpha\left(\frac{\partial u_1}{\partial\eta}\frac{\partial\bar{\eta}}{\partial\alpha}\right)_{\bar{s}}+\epsilon\left(\frac{\partial u_1}{\partial\eta}\frac{\partial\bar{\eta}}{\partial\epsilon}+UR\frac{\partial\bar{\eta}}{\partial\alpha}\right)_{\bar{s}}\right] \tag{28}$$

Expression (28) represents clockwise vorticity shed at the top separation point. At the bottom separation point, the amount of counterclockwise vorticity shed is also represented by equation (28), if subscripts $\bar{s}$ are replaced by $\underline{s}$.

Therefore, equating the net discharge of vorticity to zero,

$$\left.\begin{aligned}0=&\frac{1}{2}\left[(u_1^2)_{\bar{s}}-(u_1^2)_{\underline{s}}\right]+\frac{1}{2}\Delta\alpha\left[\left(\frac{\partial u_1^2}{\partial\eta}\frac{\partial\bar{\eta}}{\partial\alpha}\right)_{\bar{s}}-\left(\frac{\partial u_1^2}{\partial\eta}\frac{\partial\underline{\eta}}{\partial\alpha}\right)_{\underline{s}}\right]+\\&\epsilon\left\{\frac{1}{2}\left[\left(\frac{\partial u_1^2}{\partial\eta}\frac{\partial\bar{\eta}}{\partial\epsilon}\right)_{\bar{s}}-\left(\frac{\partial u_1^2}{\partial\eta}\frac{\partial\underline{\eta}}{\partial\epsilon}\right)_{\underline{s}}\right]+U\left[\left(Ru_1\frac{\partial\bar{\eta}}{\partial\alpha}\right)_{\bar{s}}-\left(Ru_1\frac{\partial\underline{\eta}}{\partial\alpha}\right)_{\underline{s}}\right]\right\}+\ldots\end{aligned}\right\} \tag{29}$$

In the quasi-steady flow, $(u_1)_{\bar{s}}=(u_1)_{\underline{s}}$, and the coefficient of $\Delta\alpha$ must be zero. Therefore, the coefficient of ϵ in equation (29) must vanish:

$$\left(\frac{\partial u_1}{\partial\eta}\frac{\partial\bar{\eta}}{\partial\epsilon}\right)_{\bar{s}}-\left(\frac{\partial u_1}{\partial\eta}\frac{\partial\underline{\eta}}{\partial\epsilon}\right)_{\underline{s}}+U\left[\left(R\frac{\partial\bar{\eta}}{\partial\alpha}\right)_{\bar{s}}-\left(R\frac{\partial\underline{\eta}}{\partial\alpha}\right)_{\underline{s}}\right]=0$$

or

$$\left(\frac{\partial q/\partial\eta\;\partial\bar{\eta}/\partial\epsilon}{R\;\partial\bar{\eta}/\partial\alpha}\right)_{\bar{s}}\left[1-\left(\frac{\partial\bar{\eta}/\partial\alpha}{\partial\bar{\eta}/\partial\epsilon}\right)_{\bar{s}}\left(\frac{\partial\underline{\eta}/\partial\epsilon}{\partial\underline{\eta}/\partial\alpha}\right)_{\underline{s}}\right]+1-\frac{(R\;\partial\underline{\eta}/\partial\alpha)_{\underline{s}}}{(R\;\partial\bar{\eta}/\partial\alpha)_{\bar{s}}}=0 \tag{30}$$

Equations (23), (25), and (30) and table I suffice to determine γ (which appears in eq. (25)). The result is,

$$\gamma=-6.1 \tag{31}$$

Definition of separation point.—In effect, it has been assumed that, during the unsteady motion, separation is defined by the condition of zero shear ($\kappa=-0.1567$) and the subsequent appearance of reverse flow relative to the surface, just as in steady flow. This assumption is open to question. The question is how (or whether) local velocity-profile characteristics may be interpreted to identify the leading edge of a wake.

The usual steady criterion, which notes the appearance of reverse flow downstream of the point of zero shear, implies that the fluid in the wake is fixed relative to the body. If, in the unsteady case, the wake may still be regarded as fixed to the body, then it may be that the steady criterion is still applicable.

However, the present assumption of the steady definition of separation is not advanced with complete confidence. Rather, it is felt that only a suitable experiment can settle this point.

LIFT OF AIRFOIL

The steady lift coefficient of the airfoil of figure 1 is determined from the steady circulation:

$$C_L^{(0)}=\frac{\rho U\Gamma}{\frac{1}{2}\rho U^2(2l)}=\frac{\Gamma}{Ul}=2\pi(0.0761)=0.48 \tag{32}$$

There are two contributions to lift proportional to ϵ. From the unsteady circulation,

$$C_{L_\epsilon}^{(0)}=2\pi\gamma=-38.6 \tag{33}$$

and a further contribution is found by consideration of the remainder of the potential flow. The two components of Kelvin's impulse for the flow illustrated in figure 1 (leaving circulation out of account) are

$$I_x,\,I_y=\pi\rho Ul^2(\beta^2\cos\alpha,\,\sin\alpha)$$

(See pars. 71 and 123 of ref. 11.) Whence, the corresponding components of vector force are

$$F_x,\,F_y=\dot{\alpha}\frac{\partial I_{x,y}}{\partial\alpha}=\pi\rho Ul^2\dot{\alpha}\,(-\beta^2\sin\alpha,\,\cos\alpha)$$

and the lift is

$$L=F_y\cos\alpha-F_x\sin\alpha=\pi\rho Ul^2\dot{\alpha}\,\frac{1+\beta^2}{2}\left(1+\frac{1-\beta^2}{1+\beta^2}\cos 2\alpha\right)$$

The following lift coefficient results:

$$C_{L_\epsilon}^{(2)}=\frac{\pi}{2}(1+\beta^2)\left(1+\frac{1-\beta^2}{1+\beta^2}\cos 2\alpha\right)=3.09 \tag{34}$$

The final expression for lift combines equations (32), (33), and (34):

$$C_L=C_L^{(0)}+\epsilon(C_{L_\epsilon}^{(1)}+C_{L_\epsilon}^{(2)})$$

$$=0.48-36\frac{\dot{\alpha}l}{U} \tag{35}$$

The sign of the second term of the result of equation (35) indicates that, while angle of attack is increasing, the lift is lower than the quasi-steady value, and higher if the angle of attack is decreasing. Thus, near maximum lift, the lift curve would exhibit a counterclockwise hysteresis loop enclosing the stall point. This result is perhaps counter to expectations, because clockwise hysteresis is found experimentally for oscillating airfoils. It may be that different directions of hysteresis should be expected when the airfoil oscillates and when, as in the present study, the stream direction oscillates.

In any case, it may be shown that the overriding effect producing counterclockwise hysteresis in the present problem is the quasi-steady movement of the separation point over the top surface. As this separation point moves forward under increasing angle of attack, clockwise vorticity in the boundary layer joins the wake as the separation point passes. Accordingly, a counterclockwise airfoil circulation (negative γ) is required to balance this effect. The term of equation (26) that is concerned with this movement is the one involving $d\bar{s}/dt$.

For the elliptic airfoil problem treated herein, the quasi-steady movement of the upper separation point is quite extensive; numerically, $\partial\bar{\eta}/\partial\alpha=13.9$, indicating that the separation point is very loosely fixed to the airfoil suface. By way of contrast, in the case of the rotating circular cylinder, there is no effect of this sort, because a change in angle of attack produces no quasi-steady movement of the separation point at all. Other contributions to the shedding of vorticity then lead to the result of clockwise hysteresis for the circular cylinder.

LIFT HYSTERESIS

The foregoing analysis does not provide a complete theory of unsteady flow about a stalled airfoil. Rather, the analysis illustrates the considerations that would underlie such a theory and further make plausible the general assumption of an expansion of lift coefficient in the form of equation (35). This expansion would be valid for nearly quasi-steady conditions. Also, it has been shown that a counterclockwise hysteresis loop may be expected at a nominal condition of maximum lift with, apparently, a large amplitude.

If the foregoing conditions are met, and $\Delta\alpha$ is simple harmonic,

$$\Delta\alpha \propto \sin 2\pi\omega t \tag{36a}$$

then

$$\dot{\alpha} \propto -2\pi\omega \sin(2\pi\omega t-90°) \tag{36b}$$

Use of relation (36b) in the lift formula (35) may be said to correspond to the assumption (ref. 5) of a positive lift-curve slope and a phase lag, 90° in this case, though the positive slope would not correspond to the steady lift curve. The hysteresis loop for this case appears as an ellipse on the lift curve of figure 6 (a). The amplitude and width of the loop are assumed small in the present discussion and are exaggerated in figure 6.

If α is not simple harmonic, then the concept of phase lag is altogether inappropriate. For example, if α is more nearly a "saw-tooth" function of time (fig. 6 (b)), then the lift increment is nearly a "battlement" function. The corresponding hysteresis loop is nearly rectangular. If α changes according to an exponential pulse (illustrated by a Gaussian curve in fig. 6 (c)), then the hysteresis loop is egg-shaped, with the broad end to the right.

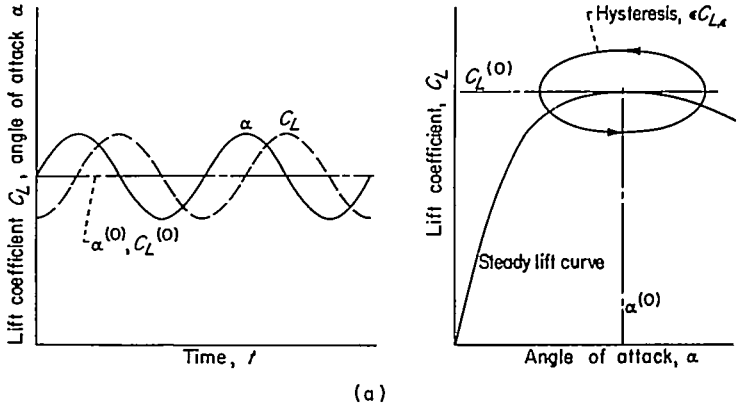

(a) Harmonic $\alpha(t)$.

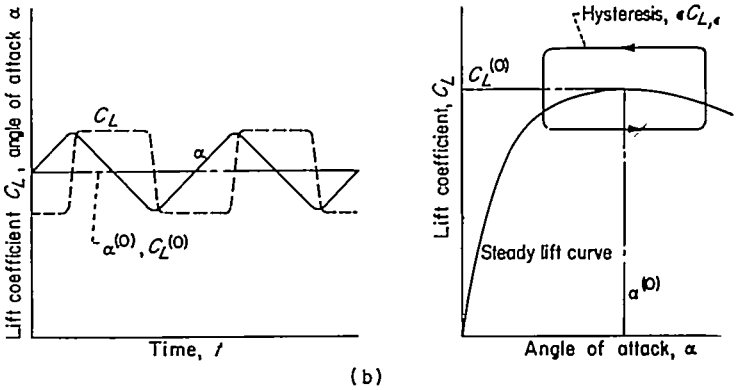

(b) "Saw-tooth" function $\alpha(t)$.

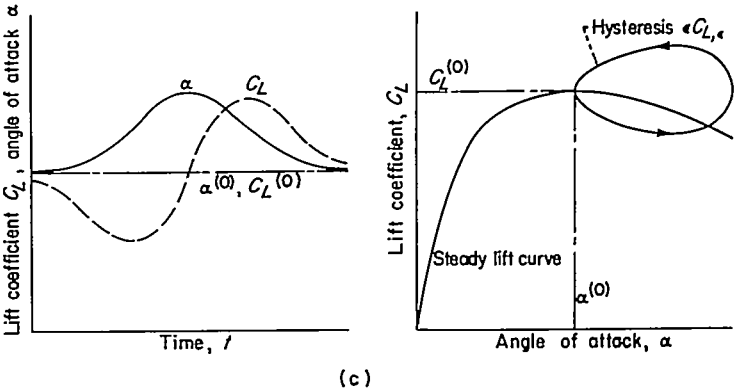

(c) Exponential pulse $\alpha(t)$.

FIGURE 6.—Variation of lift coefficient and angle of attack with time and with each other.

CONCLUSIONS

The analysis of rotating stall in an axial-flow compressor requires specification of a dynamic lift curve applicable near stall. It has previously been suggested that unsteady lift hysteresis is an important characteristic of such a curve.

Consideration of the familiar experimental fact of Magnus lift on a rotating cylinder indicates a theoretical approach to the question of aerodynamic hysteresis which, though certainly not definitive, may prove helpful. The accepted explanation of Magnus lift is that, if the cylinder is in motion toward the left and rotates clockwise, the movement of the surface delays boundary-layer separation on the top and advances it on the bottom. In steady flow, considerations of constancy of wake circulation require that the outer velocity at the two separation points be equal. The delayed separation at the top implies a lower velocity (vice versa on the bottom), and a compensatory clockwise circulation must therefore occur.

The foregoing reasoning is extended to apply to the problem of an airfoil of elliptic section in a stream of constant velocity but of (slightly) oscillating direction. The airfoil is considered to be nominally at maximum lift. This assumption, reasonable for unsteady problems at nearly stalled conditions, provides an essential simplification. To first order in small quantities, the lift (circulation) increment due to the oscillation can depend only on rate of change of angle of attack; and, just as in the cylinder case, all induced wake effects may be ignored.

For purposes of computing the amount of vorticity shed into the wake, the separation point is identified as the point of vanishing shear, just as in steady flow. It is not clear, however, that this assumption is proper.

Under these various assumptions, the unsteady increment in lift coefficient of the ellipse is found to be $-36\ \dot{\alpha}l/U$, of which about 92 percent is due to the unsteady movement of the separation points and the remainder is due to impulsive pressure. This lift increment gives the amplitude of a lift-hysteresis loop at maximum lift. The loop is counterclockwise, a result that can be related to the extremely migratory tendency of the separation point on the upper surface of the ellipse under a change in angle of attack in steady flow.

Finally, assuming oscillations of low reduced frequency, certain observations may be made concerning the shapes of hysteresis loops, and the validity of the idea of a viscous time lag in connection with unsteady lift: If the angle of attack undergoes harmonic oscillation, then the lift increment is also harmonic with a 90° phase lead or lag, depending on the sign used in the definition of C_{l_ϵ}. In this case, the hysteresis loop is elliptic. If the angle of attack varies in a nonharmonic manner, then the variation of lift does not have the same dependence on time, and the idea of time lag is inappropriate.

LEWIS FLIGHT PROPULSION LABORATORY
NATIONAL ADVISORY COMMITTEE FOR AERONAUTICS
CLEVELAND, OHIO, *August 17, 1955*

APPENDIX

SYMBOLS

The following symbols are used in this report:

A, a functions of η (eqs. (7))
B, b functions of η (eqs. (9))
C, c functions of η (eqs. (19b))
C_L lift coefficient
C_{L_α} rate of change of lift coefficient with angle of attack α
$C_{L_{\dot\alpha}}$ rate of change of lift coefficient with $\dot\alpha$
d function of η (eq. (20b))
F universal function for boundary-layer calculation (eq. (5a))
f_1 universal function for boundary-layer calculation (eq. (13))
L lift
l semichord of elliptic cylinder (fig. 1)
n coordinate measured normal to surface (eqs. (6), (36))
q dimensionless outer velocity, $\equiv u_1/U$
R function of η (eq. (3))
s dimensionless coordinate measured along surface of ellipse (fig. 1)
t time
U stream velocity (a constant)
u velocity parallel to surface
W function related to unsteady boundary layer (eq. (15)), $\equiv qZ_\epsilon$
X function related to unsteady boundary layer (eq. (18))
x Cartesian coordinate of surface of ellipse
Y function related to unsteady boundary layer (eq. (18))
y Cartesian coordinate of surface of ellipse
Z function related to momentum thickness of boundary layer (eq. (5a)), $=\frac{\theta^2 U}{\nu l}$
α angle of attack
$\dot\alpha$ time rate of change of α
$\Delta\alpha$ increment in angle of attack, $\equiv\alpha-\alpha^{(0)}$
β thickness ratio of elliptic cylinder
Γ circulation in outer flow
γ coefficient of hysteresis in circulation (eq. (10))
δ over-all thickness of boundary layer
δ^* displacement thickness of boundary layer
ϵ dimensionless angular velocity, $\equiv\dot\alpha l/U$
η coordinate on surface of ellipse (fig. 1, eq. (2))
θ momentum thickness of boundary layer
κ function for boundary-layer calculation (eq. (5a))
ν kinematic viscosity coefficient
ρ density
τ skin-friction coefficient
φ velocity potential
ω frequency

Subscripts:

$\bar s, \underline s$ evaluation at top or bottom separation point, respectively, of steady flow at maximum lift ($\alpha=\alpha^{(0)}$, $\epsilon=0$)
0 evaluation at forward stagnation point, where $q=0$
1 evaluation at outer edge of boundary layer
$\_$ evaluation at lower separation point

Subscript notation is used for partial differentiation where convenient.

Superscripts:

(0) steady conditions at maximum lift
(1) unsteady contribution due to movement of separation points
(2) unsteady contribution due to impulsive pressure
$\bar{\ }$ evaluation at upper separation point
$'$ denotes ordinary derivatives

REFERENCES

1. Mendelson, Alexander: Effect of Aerodynamic Hysteresis on Critical Flutter Speed at Stall. NACA RM E8B04, 1948. (See also Jour. Aero. Sci., vol. 16, no. 11, Nov. 1949, pp. 645–654.)
2. Farren, W. S.: Reaction on a Wing Whose Angle of Incidence is Changing Rapidly. R. & M. No. 1648, British A. R. C., 1935.
3. Halfman, Robert L., Johnson, H. C., and Haley, S. M.: Evaluation of High-Angle-of-Attack Aerodynamic-Derivative Data and Stall-Flutter Prediction Techniques. NACA TN 2533, 1951.
4. Schnittger, Jan R.: Single Degree of Freedom Flutter of Compressor Blades in Separated Flow. Jour. Aero. Sci., vol. 21, no. 1, Jan. 1954, pp. 27–36.
5. Sears, W. R.: A Theory of "Rotating Stall" in Axial Flow Compressors. Graduate School Aero. Eng., Cornell Univ., Ithaca (N. Y.). (Contract AF 33(038)–21406.).
6. Emmons, H. W., Pearson, C. E., and Grant, H. P.: Compressor Surge and Stall Propagation. Trans. A.S.M.E., vol. 77, no. 4, May 1955, pp. 455–467; discussion, pp. 467–469.
7. Marble, Frank E.: Propagation of Stall in a Compressor Blade Row. Jour. Aero. Sci., vol. 22, no. 8, Aug. 1955, pp. 541–554.
8. Moore, Franklin K.: Unsteady Laminar Boundary-Layer Flow. NACA TN 2471, 1951.
9. Howarth, L.: The Theoretical Determination of the Lift Coefficient for a Thin Elliptic Cylinder. Proc. Roy. Soc. (London), ser. A, vol. 149, no. A168, Apr. 10, 1935, pp. 558–586.
10. Goldstein, Sydney, ed.: Modern Developments in Fluid Dynamics. Clarendon Press (Oxford), 1938.
11. Lamb, Horace: Hydrodynamics. Sixth ed., Dover Pub., 1932.
12. Schlichting, Herman: Grenzschicht-Theorie. Verlag und Druck G. Braun, Karlsruhe, 1951. (Available in English translation as NACA TM 1217.)

TABLE I.—RESULTS AT SEPARATION POINTS

Quantity	Separation point ($\kappa=-0.1567$)	
	Top ($\bar s$)	Bottom ($\underline s$)
η	80. 0°	340. 83°
R	0. 985	0. 364
q	1. 210	−1. 204
q_s	0. 139	0. 137
$q_{s\alpha}$	1. 192	−7. 95
$q_{s\eta}$	−0. 0062	1. 49
Z	1. 11	0. 41
Z_α	13. 3	−5. 6
Z_η	−1. 405	0. 52
X	−55. 6	−5. 4
Y	4. 9	−4. 2